



# Magnetically trapped atoms in the vicinity of an optical nanofibre

A. Alampounti<sup>1,2</sup> · R. A. Jenkins<sup>1</sup> · S. Eriksson<sup>1</sup>

Received: 31 January 2020 / Accepted: 11 March 2020 / Published online: 31 March 2020  
© The Author(s) 2020

## Abstract

Magnetically trapped  $^{87}\text{Rb}$  atoms have been observed near a single-mode optical nanofibre. Approximately  $1 \times 10^6$  atoms were optically pumped to the  $|F = 2, m_F = 2\rangle$  state and held in the trap with a trap lifetime of up to 2 s. The temperature of the atomic sample within the magnetic trap was measured to be below  $230 \mu\text{K}$ . The compact vacuum system and high-temperature fibre feedthroughs are presented, and the feasibility of creating a quantum degenerate gas of ultracold neutral atoms near an optical nanofibre is discussed.

## 1 Introduction

Optical nanofibres (ONFs) are of significant relevance to experiments with ultracold neutral atoms due to the coupling between guided fibre modes and nearby atoms via the evanescent field. The atoms can emit light in the fibre mode [1] or scatter photons from light propagating in the fibre mode [2]. If the ONF is fabricated from one continuous fibre so that the fibre thickness along its length tapers continuously down to the thin segment and back again, light can conveniently be coupled in and out with standard photonic components via the fibre ends (pigtailed), creating a compact sub-wavelength-scale interface between the atoms and light. Low-loss tapers [3] facilitate efficient coupling of substantial light intensity into the ONF which allows manipulating atoms by the dipole force, and by cleverly utilising the azimuthal dependency of the evanescent field, arrays of single atoms can be confined very close to the ONF surface [4]. With appropriately chosen wavelengths, the confinement becomes state independent [5]. Very recently, a single collective excitation coupled to the ONF waveguide has been observed in arrays of atoms trapped near the ONF [6], leading to a nanoscale platform for waveguide quantum electrodynamics with wide-ranging applications in quantum

technology. Reviews of the topic of ONFs from the perspective of neutral atoms and quantum optics can be found in references [7, 8].

Most experiments with ultracold atoms and ONFs to date have involved comparatively small ensembles of atoms. Trapping large, dense ensembles such as Bose–Einstein condensates (BECs) near an ONF constitutes an intriguing possibility of combining the unique qualities of the ONF light–atom interface with the paradigm for creating quantum many-body systems with neutral atoms. Recent proposals involve studying superfluid flow in ring-shaped trapping potentials near ONFs [9] and complex vortex structures due to artificial magnetic fields that arise from the ONF optical field [10]. The BEC as a cold source of atoms may provide a route to realising quantum coherent tractor beams [11].

Here, we detail our efforts towards creating a quantum degenerate gas near an ONF. Our guiding design principle has been to make experimental provisions for most typical capabilities found in experiments with quantum degenerate gases, whilst allowing coupling light in and out of the pigtailed of an ONF mounted in the vacuum chamber. Our setup includes provisions to probe Feshbach resonances in ultracold alkalis such as potassium, and optical access for dipole-trapping beams and diffraction-limited imaging. These design constraints lead to a compact design and some challenges associated with handling and installing the ONF. In this article, we describe confining atoms near the ONF in a magnetic trap without a dissipative force for sufficiently long times to allow evaporative cooling. While a BEC has not yet been achieved, our work indicates that with relatively modest changes to our apparatus, degeneracy can be achieved in a trapping potential external to the ONF.

✉ S. Eriksson  
s.j.eriksson@swansea.ac.uk

<sup>1</sup> Department of Physics, College of Science, Swansea University, Singleton Park, Swansea SA2 8PP, UK

<sup>2</sup> Present Address: Department of Physics, Joint Quantum Centre (JQC), Durham-Newcastle, Durham University, Durham DH1 3LE, UK

The article is organised as follows. In Sect. 2, we provide details of the experimental setup including improved single-mode vacuum fibre feedthrough technology. In Sect. 3, we show that fluorescence from atoms can be coupled to the ONF and that atoms can be held in a magnetic trap near the fibre. We conclude with a discussion and outlook in Sect. 4.

## 2 Experimental design and setup

### 2.1 Ultrahigh-vacuum fibre feedthrough

To achieve sufficiently long trap lifetimes for evaporative cooling, the background pressure needs to be sufficiently low which in turn necessitates bakeouts at high temperatures (in our work, typically above 120°C). All components of the vacuum system, including the fibre feedthroughs must withstand the bakeout temperature. Ultrahigh-vacuum (UHV) fibre-optic feedthrough systems have been developed due to increasing applications for fibres in vacuum, including the need for multiple fibres to be passed into vacuum [12, 13]. However, many of these solutions use an epoxy to make a vacuum seal which renders the fibre fixed, increasing the time required to replace fibres if needed. Our experience is that the brittleness of ONFs leads to a susceptibility to breaking during the installation process and, therefore, the need for quick replacement is necessary. Flexibility in fibre positioning and short fibre replacement times can be achieved by the use of a fibre feedthrough setup with a compression sealing. An all-metal optical feedthrough system that can be baked to high temperatures and relies on a compression sealing has been developed [14]; however, this is a sub-optimal method for ONFs within ultracold atom experiments. An elegant hybrid compression sealing method with fibre strain relief is shown in [15]; however, this method requires a number of custom parts and significant preparation with the fibre which is unsuitable when working with delicate ONFs. Instead, we have adapted the compression sealing method outlined in [16], which we find unstable during bakeouts due to deformation of the PTFE ferrules at high temperatures, with further inspiration drawn from the work found in [17].

Our feedthrough system is made from off-the-shelf components with no customisation required and allows for a stripped or unstripped optical fibre to be passed into UHV via a narrow bore in a ferrule, creating a seal with a compression pipe fitting. The fibre is threaded through a protective PEEK sleeving across the length of the ferrule to reduce the stress exerted on the fibre due to compression. The ONF feedthrough setup is comprised of a 1/8" Swagelok pipe fitting (SS-200-1-2WBT) with a Vespel/graphite (V/Gr) ferrule (Analytical Columns C213208) and a PEEK capillary sleeve (IDEX 1581 PEEK), as shown in Fig. 1. The 1/8"

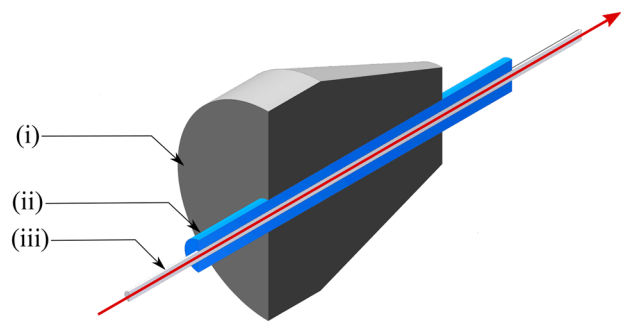


**Fig. 1** Schematic of the (i) V/Gr ferrule with a central bore to allow for the (ii) PEEK tube that houses the (iii) ONF pigtail

V/Gr ferrule has a central capillary column with a 800  $\mu\text{m}$  diameter to accommodate the PEEK tubing (254  $\mu\text{m}$  ID, 794  $\mu\text{m}$  OD), creating a tight fit for unstripped fibres with a coating diameter of 245  $\mu\text{m}$ . A vacuum seal is made when the Swagelok fitting is tightened down onto the appropriately sized ferrule and PEEK tubing, in turn compressing radially around the centrally threaded fibre.

Throughout a vacuum testing phase, cycling the temperature up to 120°C with the V/Gr ferrules or alternative PTFE-based ferrules (Analytical Columns C214208), we observed only minor differences in sealing capabilities compared between the two; however, the PTFE ferrules exhibited larger susceptibility to thermal deformation leading to vacuum leaks appearing during or after cooling down and additional stress to the fibre pigtails, as previously observed [15]. Additionally, smaller inner diameter variants of the ferrules (Analytical Columns C213204) and PEEK tube (IDEX 1572 PEEK) showed no discrepancy in the final pressure obtained in our separate vacuum testing setups but were deemed impractical as the fibre would need to be stripped to the cladding, making it more fragile. The V/Gr feedthroughs showed no change in light transmission when fully compressed to make a seal.

### 2.2 Setup for trapping ultracold atoms

The experimental setup consists of a single, compact stainless steel (SS) vacuum chamber (Kimball Physics MCF450 316LN Spherical Octagon) with two DN63CF and eight DN16CF ports. The chamber is connected at one of the DN16CF ports through a conical reducer to a six-way cross that holds a dispenser with natural Rb abundance, a 20 l/s ion pump, an ion gauge, and a non-evaporable getter (NEG) pump. A pair of magnetic coils are mounted along the axis of cylindrical symmetry above and below the chamber. The 56-mm-diameter clear bore of the magnet structure retains the clear aperture of a DN63CF viewport mounted on the top port of the chamber, and allows high-resolution imaging via a long working-distance objective (not discussed in this

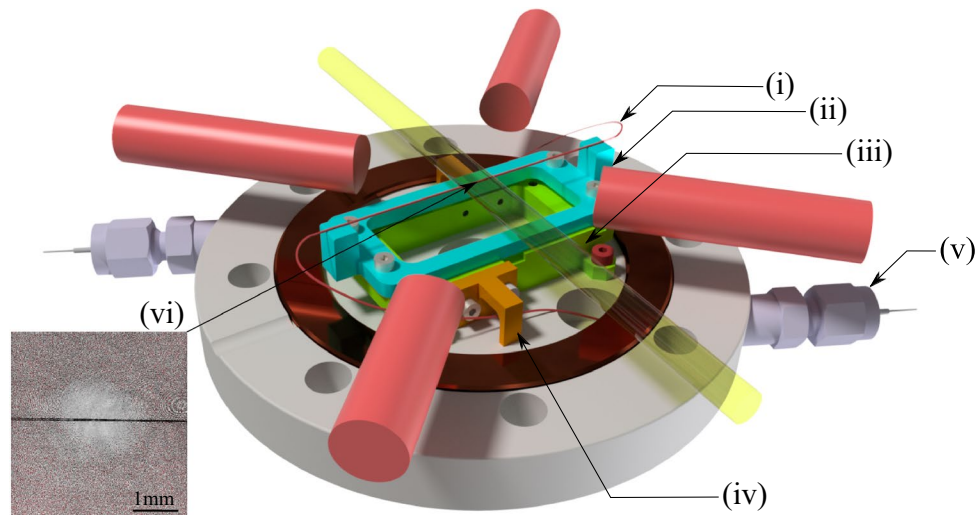


**Fig. 2** Experimental configuration of the science chamber. Design of the compact ONF mounting system with optical access for MOT beams (red) and imaging beam (yellow), angled at  $45^\circ$  and perpendicular to the ONF axis, respectively. The assembly is comprised of (i) the nanofibre (size exaggerated for clarity), (ii) the fibre holder, (iii) the fibre mounting base, (iv) the fibre pigtail guides and (v) the Swagelok fibre feedthrough system, allowing the fibre to enter through a 14-mm opening on the flange face, and (vi) magnified composite image overlay of the ONF illuminated with MOT beams (without atoms) and magnetic trap after 100 ms captured via absorption imaging

article). The size of the chamber allows for a small separation between the coils of 11 cm. In quadrupole mode, the coils are capable of generating magnetic field gradients up to 2.2 T/m, and are used in both the magneto-optical trapping (MOT) stage of the experimental sequence and for magnetic trapping. We choose magnetic trapping as a platform for evaporative cooling due to the simplicity of moving the trap centre to coincide with the thin segment of the ONF with shimming coils external to the chamber. The setup includes a far-detuned laser beam for creating dimple traps; however, in the experiments with overlapped ONF and trap centre described here, this feature was not used to avoid risking the integrity of the fibre due to accidental illumination with the high-power (5W) infrared laser. The coils are independently energised and can in principle provide a homogeneous field up to 62 mT with 400 A when operated in Helmholtz mode. Further details of the apparatus can be found in [18, 19]. In the absence of the ONF, the vacuum reaches the  $10^{-11}$  mbar range when the vacuum system is baked at  $120^\circ\text{C}$  and the NEG is activated at high temperature. Mounting the ONF restricts the bakeout temperature to  $60^\circ\text{C}$  as discussed below, degrading the vacuum to the low  $10^{-10}$  mbar range.

### 2.3 ONF mount and flange

Central to experimental configuration is a compact ONF mounting flange, schematically shown in Fig. 2. This custom-made DN63-16CF reducer flange with fibre feedthroughs is designed to allow a compact geometry of the experimental setup and is fabricated from SS316LN

for its good magnetic properties. Swagelok pipe fittings (also SS316LN) with a  $1/8''$ -diameter bore for the fibre feedthrough system are welded to the side of the flange to allow the quadrupole coils to be mounted as close to the chamber on the vertical axis as possible. The Swagelok fittings are cold welded to minimise any alteration to the magnetic properties of the flange. The flange with the fibre assembly is connected to the bottom port of the chamber. A viewport is added to the DN16CF port on the outward-facing side of the flange to allow the vertical axis MOT beam (not shown in Fig. 2) into the chamber.

The ONF is mounted on a removable U-shaped fibre holder (shown in cyan in Fig. 2) and secured using UV-curing epoxy at both ends of the ONF tapers, 60 mm apart. This assembly is fixed to the bottom flange of the vacuum chamber via an intermediate mount (green). The mount not only serves for a faster installation of the fibre holder but also sets the position of the ONF close enough to the geometric center of the quadrupole coils such that the magnetic trap can be overlapped with the ONF. The fibre pigtails are each coiled counterclockwise and passed under their respective fibre guides to maintain the bend radius of the fibre and avoid obstruction to optical beam paths. The fibre exits the flange via bore holes that tunnel through to the Swagelok fibre feedthroughs. The entire ONF mounting system has been manufactured from grade 2 titanium, chosen for its good magnetic properties and comparable thermal expansion coefficient to glass (silica) to reduce fibre strain during UHV bakeouts. The mounting structure is designed so that the MOT beams are oriented at  $45^\circ$  with respect to the ONF axis

to allow optical access for an imaging beam perpendicular to the ONF transmission axis and for further atom diagnostics.

The ONF was fabricated<sup>1</sup> using the flame-brushing technique [3, 20, 21]. The resulting single-mode fibre has a waist of approximately 400 nm, a total length of 60 mm and an average transmission rate of 97% which is unchanged when mounted. The background pressure reaches a minimum of  $3 \times 10^{-10}$  mbar after installing the ONF and baking out at the 60 °C temperature limit of the epoxy. Despite conducting the entire assembly of the ONF flange in an ISO 2 classified clean room and careful establishing of vacuum, the fibre transmission is reduced to about 70% in vacuum, with no change during heating and no discernible mechanical distortion. An online transmission test was not possible during work in the clean room and the precise timing and the origin of this loss is currently unknown. Nevertheless, we show below that light can be coupled to guided fibre modes. Further details of the experimental setup including the ONF can be found in [22].

### 3 Measurements and results

#### 3.1 Magneto-optical trapping and ONF fluorescence

A conventional MOT with retro-reflected beams is used to capture approximately  $1 \times 10^7$   $^{87}\text{Rb}$  atoms from the background vapour produced by resistively heating the dispenser. It is notable that if the ONF assembly is replaced by a blank flange, but otherwise using identical experimental parameters, the MOT captures about an order of magnitude more atoms. To gauge the quality of the ONF, the MOT is overlapped along the ONF segment and atomic fluorescence is collected through the nanofibre pigtails. In this experiment, the dispenser is kept on at a constant current until the MOT reaches a pressure equilibrium after which photons are detected with a single-photon counting module (SPCM-AQRH-14-FC) using a trigger pulse-width of 50  $\mu\text{s}$ . The number of photons in each SPCM pulse is plotted in a histogram and is shown to follow a Poissonian distribution as expected from MOT fluorescence (Fig. 3).

Correcting for the quantum efficiency of the detector and coupling efficiency of the ONF, the average count rate is estimated at 960(182) kC/s, approximately 400 kC/s above the scattering background. This is in agreement with previously published results [1].

<sup>1</sup> Fabrication and mounting to the U-shaped holder took place at the Atominstitut-TU Wien, upon which the mounted ONF was transported to Swansea for installation.

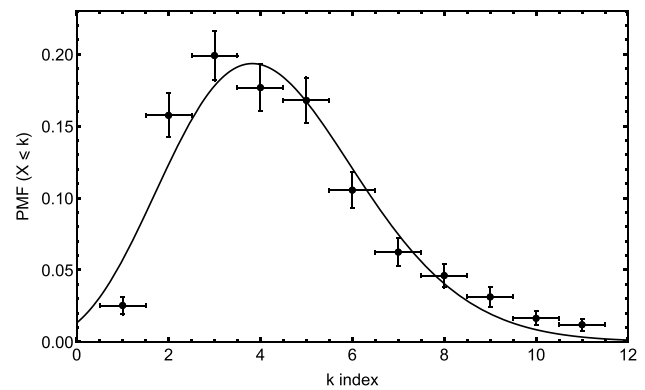


**Fig. 3** Poissonian fit of the raw fluorescence data with a bin size of 5. Normalised fluorescence data as extracted from a histogram. The Poissonian fit predicts a mean value of  $k = 4.3$  corresponding to 21.5 photons within 50  $\mu\text{s}$

#### 3.2 Magnetic trapping near the ONF

To allow the background pressure in the chamber to recover before magnetic trapping, the dispenser is operated in a pulsed mode, with a 10-s cool-down period during which the atoms are held in the MOT. Following this, the atoms are moved closer to the geometric centre of the quadrupole by increasing the field gradient linearly from  $b' = 0.135$  T/m to  $b' = 0.5$  T/m and further red-detuning of the cooling laser from  $\delta = -3.5\Gamma$  to  $\delta = -5.5\Gamma$ . Prior to the magnetic trap stage, the atoms are further cooled using a polarisation gradient optical molasses stage with the cooling laser detuned approximately at  $\delta = -15\Gamma$ . At this stage, the cloud has a temperature of  $T = 20(2)$   $\mu\text{K}$ , established via absorption imaging at increasing lengths of time-of-flight (TOF) after releasing the atoms.

The presence of magnetically trapped atoms in the vicinity of the ONF was initially verified via a MOT-recapture test as well as by direct absorption imaging of the cloud. In both cases, we optically pump the atoms on the  $F = 2 \rightarrow F' = 2$  line before loading the atoms in the magnetic trap where they are held for 300 ms with a magnetic field gradient of  $b' = 1.1$  T/m. About 40% of the initial sample is pumped to the  $|F = 2, m_F = 2\rangle$  state. For atom recapture, the magnetic trap is switched off completely and ramped up again to our MOT-optimised value after a “dark” period  $\sim 20$  ms. A control test is performed by keeping the current in the quadrupole magnets off during the magnetic trap stage. The absence of atoms in the recaptured MOT control test verifies that there is no background loading.

The lifetime of the atoms in the magnetic trap was measured on separate days using atom recapture and absorption imaging methods as shown in Fig. 4. The MOT recapture method yields a  $1/e$ -lifetime of 2.5(3) s whereas the data from absorption images yield a lifetime of 1.2(1) s. The



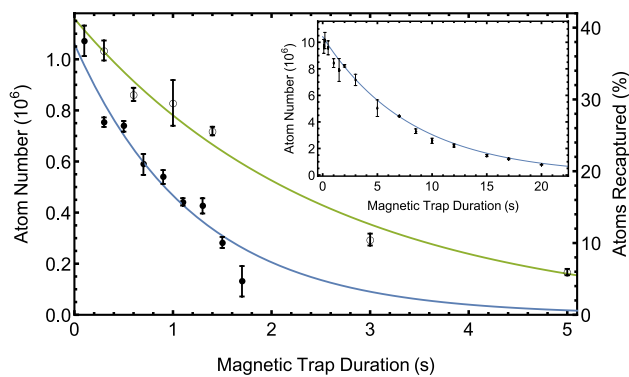


**Fig. 4** Determination of the magnetic trap lifetime through both atom recapture and absorption imaging of the magnetic trap. Open circles, right ordinate: the fractional number of atoms recaptured in a MOT as a function of magnetic trap duration. Filled circles, left ordinate: the number of atoms as a function of magnetic trap duration via absorption imaging. The green and blue curves are exponential models fit to the data (see text for details). The uncertainty is given by the standard error. The inset shows a lifetime measurement without the ONF assembly installed

decreased lifetime can be attributed to the overall deterioration of the pressure in the vacuum chamber in the intervening time between experiments, e.g. due to continuous Rb-dispensing in experiments such as fluorescence detection described above. In the absence of the ONF assembly and a higher bakeout temperature, but with otherwise similar experimental conditions, the trap lifetime increases to about 8 s as shown in the inset of Fig. 4. In this configuration, rf-evaporation works well, and shows promise in combination with a hybrid trap [19].

The temperature of the atoms in the magnetic trap was measured via a TOF-absorption imaging to be  $120(40) \mu\text{K}$  [ $230(10) \mu\text{K}$ ] along the the vertical (horizontal) axis. We note that the uncertainty in these measurements, estimated statistically from a limited number of repeats, is likely an underestimate. The quality of the absorption images in these rather dilute samples deteriorates rapidly with increasing TOF.

The absorption imaging axis is aligned with the centre of the magnetic trap such that the probe beam is orthogonal to the ONF transmission axis. The magnetically trapped atoms and the ONF waist have been imaged during the same experimental run and overlaid as shown in Fig. 2. Here, it is observed that the trapped atoms are aligned with the ONF waist in the vertical plane and the fibre transmission axis of the horizontal plane; however, with a single imaging beam the overlap between the 2-mm-diameter magnetic trap and ONF along the imaging axis cannot be fully confirmed. The 5(1)mm depth of field (DOF) of the imaging system provides a conservative upper bound for the atom–ONF overlap along the imaging axis. The experimentally measured DOF is in agreement with the numerical estimate using ray

tracing. With a large number of repetitions, enough photons scattered from the imaging beam by the atoms into a guided mode of the ONF could be collected to confirm trap–ONF overlap; however, this is beyond the scope of this study.

## 4 Discussion and outlook

In this work, we demonstrate to our knowledge the first realisation of a quadrupole magnetic trap in the vicinity of an ONF and we have shown that  $^{87}\text{Rb}$  atoms can be confined in the trap. We can detect MOT fluorescence at the output of the ONF. We show that an ONF can be integrated with an apparatus that contains all experimental elements necessary for creating and probing a quantum degenerate gas.

The currently achieved trap lifetime and phase-space density are likely to be too restrictive for reaching quantum degeneracy with standard rf-evaporation schemes in our setup, but may, in combination with preventing unwanted spin-flips near the quadrupole centre by creating a repulsive optical potential with a guided ONF mode, already allow small cold samples for observing the quantum coherent tractor beam effect [11]. The lower lifetime is consistent with increased trap loss due to collisions with the background gas arising from the poorer vacuum that is achieved at the lower bakeout temperatures imposed by the fibre mounting. Indeed, we predicted this outcome and successfully mounted an ONF using a high-temperature UV curing epoxy (EPO-TEK 353ND) during our ONF fabrication phase. Unfortunately, the fibre pigtailed of this sample failed due to an accidental contact with the chamber wall during the installation process.

Without invasive action, degeneracy could be reached by loading into a pure optical trap or hybrid trap with access to faster evaporation rates [23–25]. The capability to create hybrid traps already exists in our setup. However, more work is needed to control the dipole beam to bring the trap closer to the ONF. Preliminary work indicates a weak improvement in the trap lifetime by moving the magnetic trap centre away from the ONF, but more work is needed to understand this effect. The use of a second orthogonal imaging axis or measuring the absorption of probe light coupled into the ONF can be used to probe trap–ONF overlap.

The reduced number of atoms in the MOT with the ONF flange present is likely to be caused by a change in vacuum dynamics during dispenser pulsing. In the current mounting orientation, the ONF assembly obscures the orifice via which atoms enter the chamber. In future improvements, a better orientation could be used, or a somewhat larger chamber size could be employed at the expense of some loss of magnetic field gradient or magnitude. A larger chamber would greatly reduce the likelihood of damaging the fibre pigtailed during assembly. Ideally, the atoms would be loaded

from a cold source in a separate chamber as is already the practice in many experiments. This configuration would also improve the trap lifetime, at the expense of only moderately increasing experimental complexity.

In summary, our work constitutes a first step towards a BEC–ONF interface. We have identified the most obvious technical obstacles which currently prevent efficient evaporative cooling in a trap at some distance away from the ONF. Further work will be necessary to investigate the effect of bringing a cold dense sample closer to the ONF.

**Acknowledgements** We are grateful to Arno Rauschenbeutel and his group for making their ONF fabrication facility available, Thomas Hoinkes for assistance during fabrication, and the invaluable discussion on the topic of ONFs we have held. We thank Julian Kivell and Phil Hopkins for expert technical support during manufacturing. This work was supported by the UK EPSRC via the Swansea University Doctoral Training Partnership.

**Open Access** This article is licensed under a Creative Commons Attribution 4.0 International License, which permits use, sharing, adaptation, distribution and reproduction in any medium or format, as long as you give appropriate credit to the original author(s) and the source, provide a link to the Creative Commons licence, and indicate if changes were made. The images or other third party material in this article are included in the article's Creative Commons licence, unless indicated otherwise in a credit line to the material. If material is not included in the article's Creative Commons licence and your intended use is not permitted by statutory regulation or exceeds the permitted use, you will need to obtain permission directly from the copyright holder. To view a copy of this licence, visit <http://creativecommons.org/licenses/by/4.0/>.

## References

1. K.P. Nayak, P.N. Melentiev, M. Morinaga, F.L. Kien, V.I. Balykin, K. Hakuta, *Opt. Express* **15**, 5431 (2007)
2. G. Sagué, E. Vetsch, W. Alt, D. Meschede, A. Rauschenbeutel, *Phys. Rev. Lett.* **99**, 163602 (2007)
3. F. Warken, E. Vetsch, D. Meschede, M. Sokolowski, A. Rauschenbeutel, *Opt. Express* **15**, 11952 (2007). <https://doi.org/10.1364/OE.15.011952>
4. E. Vetsch, D. Reitz, G. Sagué, R. Schmidt, S.T. Dawkins, A. Rauschenbeutel, *Phys. Rev. Lett.* **104**, 203603 (2010). <https://doi.org/10.1103/PhysRevLett.104.203603>
5. A. Goban, K.S. Choi, D.J. Alton, D. Ding, C. Lacroûte, M. Pototschnig, T. Thiele, N.P. Stern, H.J. Kimble, *Phys. Rev. Lett.* **109**, 033603 (2012). <https://doi.org/10.1103/PhysRevLett.109.033603>
6. N.V. Corzo, J. Raskop, A. Chandra, A.S. Sheremet, B. Gouraud, J. Laurat, *Nature* **566**, 359 (2019). <https://doi.org/10.1038/s41586-019-0902-3>
7. T. Nieddu, V. Gokhroo, S. NicChormaic, *J. Opt.* **18**, 053001 (2016). <https://doi.org/10.1088/2040-8978/18/5/053001>
8. P. Solano, J.A. Grover, J.E. Hoffman, S. Ravets, F.K. Fatemi, L.A. Orozco, S.L. Rolston, *Adv. At. Mol. Opt. Phys.* **66**, 439 (2017)
9. R. Sachdeva, T. Busch, *Phys. Rev. A* **95**, 033615 (2017). <https://doi.org/10.1103/PhysRevA.95.033615>
10. J. Schloss, P. Barnett, R. Sachdeva, T. Busch, [arXiv:1910.02364](https://arxiv.org/abs/1910.02364) (2019)
11. M. Sadgrove, S. Wimberger, S. NicChormaic, *Sci. Rep.* **6**, 28905 (2016). <https://doi.org/10.1038/srep28905>
12. J.D. Weiss, J.H. Stoeber, *Appl. Opt.* **24**, 2755 (1985)
13. J. Cowpe, R. Pilkington, *Vacuum* **82**, 1341 (2008)
14. D.L. Miller, N.T. Moshegov, *J. Vac. Sci. Technol. A* **19**, 386 (2001)
15. B. Buchholz, V. Ebert, *Rev. Sci. Instrum.* **85**, 055109 (2014)
16. E.R. Abraham, E.A. Cornell, *Appl. Opt.* **37**, 1762 (1998)
17. T. Reinsch, C. Cunow, J. Schrötter, R. Giese, *Meas. Sci. Technol.* **24**, 3 (2013). <https://doi.org/10.1088/0957-0233/24/3/037001/pdf>
18. C.I. Laidler, Ph.D. thesis, Swansea University (2013)
19. R. Jenkins, Ph.D. thesis, Swansea University (2016)
20. L. Tong, R.R. Gattass, J.B. Ashcom, S. He, J. Lou, M. Shen, I. Maxwell, E. Mazur, *Nature* **426**, 816 (2003)
21. G. Brambilla, V. Finazzi, D.J. Richardson, *Opt. Express* **12**, 2258 (2004)
22. C.A. Alampounti, Ph.D. thesis, Swansea University (2019)
23. R. Roy, A. Green, R. Bowler, S. Gupta, *Phys. Rev. A* **93**, 043403 (2016). <https://doi.org/10.1103/PhysRevA.93.043403>
24. J. Hu, A. Urvoy, Z. Vendeiro, V. Crépel, W. Chen, V. Vuletić, *Science* **358**, 1078 (2017)
25. Y.J. Lin, A.R. Perry, R.L. Compton, I.B. Spielman, J.V. Porto, *Phys. Rev. A* **79**, 063631 (2009). <https://doi.org/10.1103/PhysRevA.79.063631>

**Publisher's Note** Springer Nature remains neutral with regard to jurisdictional claims in published maps and institutional affiliations.